BASIC SCIENCE

Nanomedicine: Nanotechnology, Biology, and Medicine
10 (2014) 1065–1073

Original Article

nanomedjournal.com

The arrhythmogenic effect of self-assembling nanopeptide hydrogel scaffolds on neonatal mouse cardiomyocytes

Yu-Wei Chiu, MD[a,c], Wen-Pin Chen, PhD[b], Chi-Chang Su, MS[a], Yen-Chia Lee, MS[a], Pei-Hsing Hsieh, MS[a], Yi-Lwun Ho, MD, PhD[c,d,*]

[a]*Division of Cardiology, Department of Internal Medicine, Far-Eastern Memorial Hospital, New Taipei City, Taiwan*
[b]*Institute of Pharmacology, School of Medicine, National Taiwan University, Taipei, Taiwan*
[c]*Graduate Institute of Clinical Medicine, National Taiwan University Hospital and National Taiwan University College of Medicine, Taipei, Taiwan*
[d]*Division of Cardiology, Department of Internal Medicine, National Taiwan University Hospital and National Taiwan University College of Medicine, Taipei, Taiwan*

Received 14 June 2013; accepted 22 January 2014

Abstract

The chaotic spatial disarray due to extracellular matrix expansion disrupts cardiomyocytes interaction and causes arrhythmia. We hypothesized that disordered nanopeptide scaffolds can mimic the chaotic spatial disarray related to cardiac fibrosis and have arrhythmogenic effects on cardiomyocytes. Primary mouse cardiomyocytes were cultured in 2D traditional and 3D nanopeptide hydrogel scaffold systems. Cardiomyocytes in 3D scaffolds showed irregular spontaneous contractile activity as compared with 2D culture controls. Calcium fluorimetric imaging revealed that basal intracellular calcium level increased 1.42-fold in cardiomyocytes cultured in the 3D scaffold, in vitro. The mRNA levels of sarcoplasmic reticulum calcium transport ATPase, ryanodine 2 receptor and connexin 43 elevated 2.14-fold, 2.33-fold and 2.62-fold in 3D compared with 2D. Immunofluorescence imaging revealed lateralization of the distribution of connexin 43 in 3D group. These findings suggest that 3D hydrogel culture system provides a model for the development of cardiac dysrhythmia. These limitations should be considered during cardiac tissue engineering.

From the Clinical Editor: This team of scientists has established a unique 3D hydrogel culture system as a model for the development of cardiac dysrhythmia.

Key words: *Cardiomyocyte*; *Nanopeptide scaffold*; *Arrhythmia*; *Connexin 43*

Recently, three-dimensional (3D) culture environments for cardiac tissue engineering have become a promising field. In vivo tracking of direct intracoronary or intramyocardium injected stem cells revealed that less than 10% of the cells were retained in the injured heart because of the hostile environment.[1,2] An active area of new strategies to repair cardiac damage is the development of appropriate 3D culture environments amenable to cardiac cell expansion and functional activity. In normal heart tissue, the cardiomyocytes are surrounded by fibroblasts and the extracellular matrix which offer mechanical support, regulate metabolism and homeostasis, remodel and interact with the cardiomyocytes.[3] With a combination of cells, regulating factors, and a scaffold, the 3D culture system could be used for cell expansion, to increase functional activity, and to repair the infarcted myocardium. Lionetti et al showed that hyaluronan mixed esters rescued infarcted rat hearts by improving vascularization, cardiomyocyte survival, and tissue function without the need of stem cell transplantation.[4] Lin et al reported that intramyocardial peptide nanofiber injection improved bone marrow cell retention and cardiac functions after myocardial infarction in pigs.[5] These encouraging results render 3D scaffolds as a promising material for cardiac repair and regeneration.

Disclosures: All of the authors disclose no conflict of interest.

This study was supported by Far Eastern Memorial Hospital National Taiwan University Hospital Joint Research Program (grant no. 101-FTN11, 102-FTN02), Smart-Health Technology Research & Development Center of National Taiwan University (grant no. 10R71608-1/101R7608-1), Taiwan National Science Council (grant no. NSC 100-2314-B-002-114-MY3), and the Center for Dynamical Biomarkers and Translational Medicine, National Central University, Taiwan (grant no. NSC 100-2911-I-008-001).

* Corresponding author. Graduate Institute of Clinical Medicine, Division of Cardiology, Department of Internal Medicine, National Taiwan University Hospital and National Taiwan University College of Medicine, Taipei 10016, Taiwan.

E-mail address: ylho@ntu.edu.tw (Y.-L. Ho).

http://dx.doi.org/10.1016/j.nano.2014.01.005

While developing a proper 3D scaffold for regenerative medicine, physical and mechanical properties of scaffolds are crucial as they must provide a suitable environment for cell attachment, proliferation, differentiation, and diffusion of nutrients and waste products. Moreover, such correct 3D organization for proper cell-cell interaction is also important. The increase in extracellular matrix proteins enlarges the intracellular space and causes delayed electric signal transduction between cells, which increases the possibility of arrhythmia.[6,7] Accumulation of extracellular collagen leads to excessive atrial fibrosis and maintenance of atrial fibrillation.[8] In addition to the excess extracellular collagen quantity, the disarray alignment of collagen fibers will also increase the severity of atrial fibrillation.[9,10] In a 3D system, the cell alignment, cell-cell contact, and the interaction with scaffolds are distinct from those in the traditional 2D culture method.[11] Altered 3D organization may have an influence on cell development and cause different cell behavior, which should be taken into consideration.

BD™ PuraMatrix™ Peptide Hydrogel is a synthetic matrix that is used to create 3D microenvironments for cell culture. It consists of standard amino acids (1% w/v) and 99% water. Under physiological conditions with monovalent cations, the peptide component self-assembles into a 3D hydrogel that exhibits a water–soluble β-sheet nanometer-scale fibrous structure with irregular sized holes. It has been shown to promote the differentiation of various cell types, including hepatocyte progenitor cells, hippocampal neurons, and endothelial cells,[12–15] and has been used in cell proliferation, migration, invasion, and tissue regeneration studies.

Cardiomyocytes in normal myocardial tissue are electrically coupled primarily in an end-to-end fashion by intercellular gap-junction complexes. The chaotic spatial disarray due to extracellular matrix expansion disrupts this convention during cardiac fibrosis. We hypothesized that disorderly nanopeptide scaffolds can mimic the chaotic spatial disarray related to cardiac fibrosis and have an arrhythmogenic effect on cardiomyocytes. Differ from other ordered 3D anisotropic scaffolds, self-assembling BD™ PuraMatrix™ Peptide Hydrogel builds random 3D structure and is chosen to mimic irregular extracellular matrix alignment. Subsequently, primary neonatal mouse cardiomyocytes were cultured in the peptide hydrogel to address the following objectives: (1) observe cardiomyocyte proliferation and contraction function; (2) determine B-type natriuretic peptide and intracellular calcium concentrations; (3) examine the mRNA expression of calcium channel proteins, calcium homeostasis related proteins, and connexin 43 (CX 43, a gap junction protein); and (4) compare the gap junction protein intracellular distribution in 3D and 2D culture systems.

Methods

Primary neonatal mouse cardiomyocyte (NMC) isolation and culture

Neonatal B6 mice (1–3 days old) were sacrificed by decapitation. All experimental protocols are approved by the Far-Eastern Memorial Hospital Animal Care and Use Committee. The hearts were immediately excised and transferred into ice-cold phosphate buffer saline (PBS) (Sigma-Aldrich, St Louis, USA), and quickly minced in collagenase A + B (Roche, Basel, Switzerland) solution (10 mg/mL in PBS). After incubation for 30 min at 37 °C, the attached fibroblasts on the dish were removed, and cardiomyocytes in the supernatants were resuspended in Claycomb medium with 10% fetal bovine serum (FBS) (Gibco, New York, USA) and pre-plated for 90 min at 37 °C to reduce the number of fibroblasts and endothelial cells in the final cardiomyocyte suspension. The cardiomyocytes were cultured on gelatin/fibronectin-coated tissue-culture flasks in Claycomb medium at 37 °C in a CO_2 incubator. Cells harvested and cultured in this method served as the 2D control group.

Preparation of BD™ PuraMatrix™ Peptide Hydrogel

The BD™ PuraMatrix™ Peptide Hydrogel forms a fiber network with a pore size of 50–200 nm, expected nanofibers range from 5 to 30 nm (BD Biosciences PuraMatrix product information sheet, www.puramatrix.com), closely resembling the structure of the extracellular matrix. At a gel concentration of 0.5%, The BD™ PuraMatrix™ Peptide Hydrogel possesses low mechanical strength and allows for cell migration within the gel. A 0.5% hydrogel cell carrier was prepared by mixing the following components in a 2:1:1 ratio: 1% stock solution of BD™ PuraMatrix™ Peptide Hydrogel (BD hydrogel; BD Biosciences, USA), 20% sucrose (Sigma-Aldrich, Sweden AB), and DMEM containing Ca2+ and Mg2+. For the preparation of the 3D cardiomyocyte culture, cardiomyocytes were detached from the culture flasks with 0.25% trypsin-EDTA, washed, and assessed for viability with trypan blue (Sigma-Aldrich Sweden AB, Stockholm, Sweden). The cardiomyocytes were concentrated in complete Claycomb medium. The PuraMatrix™ Peptide Hydrogel was immersed in complete Claycomb medium containing the cardiomyocytes.

Morphological assessment with scanning electron microscopy

Cardiomyocytes contained in PuraMatrix were culture for 3 days in Claycomb medium and then fixed with glutaraldehyde (4% in PBS) overnight, rinsed with PBS, and subsequently dehydrated in acetone with increasing concentrations (75%, 85%, 95%,100%). Specimens were then vacuum-dried for about 6 h and coated with gold with a sputter coater (Technics Hummer-II). Pictures were taken with a Hitachi S-800 (Tokyo, Japan) scanning electron microscope.

Cell proliferation assay

Cell viability was analyzed at the indicated times. All cell cultures were incubated in complete Claycomb medium with 10% FBS and antibiotics under 5% CO_2 at 37 °C. The cardiomyocytes (5×10^4 cells/well) were seeded on the nanofiber scaffold or gelatin/fibronectin-coated 12-well dishes. The cell proliferation was monitored by the WST-1 assay from day 1 to 11 with a microplate reader (BioTek, μQuant Microplate Spectrophotometer).

Measurement of calcium transients

Freshly isolated primary neonatal mouse cardiomyocytes were plated (5×10^5 cells/well) on gelatin/fibronectin-coated

35-mm glass-bottomed dishes or peptide hydrogel and allowed to grow for 3 days prior to testing. The media were replaced daily. On day 3, intracellular calcium transients were measured by IonOptix system (IonOptix, Milton, MA, USA). Briefly, cells were then loaded with 5 μM fura-2 AM at room temperature for 30 min in Claycomb medium, followed by 2 rinses in medium and a 30-min incubation to allow full cleavage of fura-2 AM to fura-2, a fluorescent calcium ion indicator substance which undergoes a shift in its excitation spectrum as it binds to calcium. Fura2-loaded myocytes on glass-bottom dish were mounted on a flow chamber on the stage of an inverted Nikon Ti microscope. The cells were observed using a 40x objective and perfused with Tyrode-HEPES buffer at 2 ml/min at 37 ± 1 ° C through a Warner in-line heater associated with an automatic temperature controller (TC-344b, Warner Instrument Co.). The constituents of Tyrode-HEPES buffer were (in mM, pH 7.4): 135 NaCl, 5.4 KCl, 0.35 NaH_2PO_4, 10 HEPES, 1.2 $CaCl_2$, 1 $MgCl_2$ and 10 glucose. Fura2-loaded cell was exposed to the alternating excitation wavelengths of 340 and 380 nm controlled by IonOptix Hyperswitch Light Source System that uses a galvanometer-driven mirror to steer light between the two filters with the rates up to 1000Hz. With the use of a photomultiplier tube (PMT), intracellular calcium signal can be quantified by a ratio between the intensity levels of the resultant fluorescent emission (F340/F380) and ratio rates as high as 250 ratio pairs per second are achievable. The indices of fura2 Ca2+ ratiometric signal (F340/F380) used to describe the Ca2+ transient were basal level, the amplitude of calcium transient, and area under calcium transient. All parameters were analyzed off-line using IonWizard (IonOptix, Milton, MA, USA).

TaqMan quantitative real-time reverse transcription PCR

Cardiomyocyte RNA was isolated using the TRIzol (Invitrogen, New York, USA) method and then transcribed to cDNA using the High Capacity cDNA Reverse Transcription Kit (Invitrogen, New York, USA). Real-time PCR was performed with TaqMan probes and primers from Invitrogen on the T-type calcium channel genes *Cav3.1* (Assay ID: Mm00486549_m1) and *Cav3.2* (Assay ID: Mm00445369_m1), the L-type calcium channel gene *CACNA1C* (Assay ID: Mm_01188822_m1), and the gap junction gene *CX 43* (Assay ID: Mm00439105_m1). GAPDH (Assay ID: Mm99999915_g1) served as the control for normalization. qPCR reactions were performed with the TaqMan Gene Expression Master Mix Kit (Invitrogen, New York, USA). Reactions were run on a Roche LightCycler® 480 Real-Time PCR System. Relative gene-expression values were calculated by the $2^{-\Delta Ct}$ method.

RNA microarray assay

Total RNA (0.2 μg) was amplified from 10 wells of cell culture by a Low Input Quick-Amp Labeling kit (Agilent Technologies, USA) and labeled with Cy3 (CyDye, Agilent Technologies, USA) during the in vitro transcription process. Cy3-labled cRNA (0.6 μg) was fragmented to an average size of 50–100 nucleotides by incubation with fragmentation buffer at 60 °C for 30 min. The corresponding fragmented and labeled cRNA was then pooled and hybridized to Agilent SurePrint G3 Mouse GE 8 × 60 K Microarray (Agilent Technologies, USA) at 65 °C for 17 h. After washing and then blow drying with a nitrogen gun, microarrays were scanned with an Agilent microarray scanner (Agilent Technologies, USA) at 535 nm for Cy3. Scanned images were analyzed by Feature Extraction Software, version 10.5.1.1 (Agilent Technologies, USA).

Immunofluorescence stain

Representative cultures from 2D and 3D cultures were fixed in formalin, permeabilized with 0.1% Triton X-100, blocked in 10% BSA, and stained with anti-connexin 43 (1:200) rabbit polyclonal antibody (Cell Signaling Technologies, USA) followed by a goat anti-rabbit Alexa Fluor 488 (1:1000) antibody (Invitrogen, New York, USA). Samples were stained with Alexa Fluor 594-conjugated anti-Troponin I heavy chain (Santa Cruz Biotechnology, Dallas, USA); all scaffolds were counterstained with DAPI (Invitrogen, New York, USA) to visualize cell nuclei and imaged using a Zeiss LSM 510 multiphoton confocal microscope (Carl Zeiss Microscopy, New York, USA) or IX51 (Olympus).

Enzyme-linked immunosorbent assay

Primary neonatal mouse heart cell culture medium was measured by ELISA. Briefly, 96-well plates were coated with an anti-mouse B type natriuretic peptide (BNP) antibody (Abnova). The anti-BNP antibody was added and incubated at room temperature for 2 h. Claycomb culture medium was added and incubated for 2.5 h. A streptavidin-horseradish peroxidase (HRP) solution was added and incubated at room temperature for 45 min followed by addition of a substrate solution. The optical density in the wells was monitored by a microplate reader (BioTek, μQuant Microplate Spectrophotometer) at a wavelength of 450 nm.

Statistical analysis

The experiments were repeated 5 times to get the mean and for the statistical analysis. All continuous results were expressed as the mean ± standard deviation (SD). Comparisons between groups for continuous data were made using Student's *t* test. A p value of <0.05 was considered statistically significant.

Results

Cell proliferation assay

Both the 3D hydrogel nanopeptide scaffold and the traditional 2D control scaffold supported cardiomyocyte attachment, proliferation, and metabolic activity. Significant increases in cell number over time were observed through day 7 for both groups, suggesting that nanopeptide scaffolds provide a 3D microenvironment amenable to cardiomyocyte culture and expansion. The 2D culture system reached the expansion limit, but the 3D system had a higher capacity for cell proliferation after 7 days (Figure 1). Both the 2D and 3D systems supported metabolically active and contractile cardiomyocytes up to 14 days in culture.

Cardiomyocyte in PuraMatrix Peptide Hydrogel

Immunofluorescence staining was performed to study cardiomyocytes assembly in 2D and 3D culture system first.

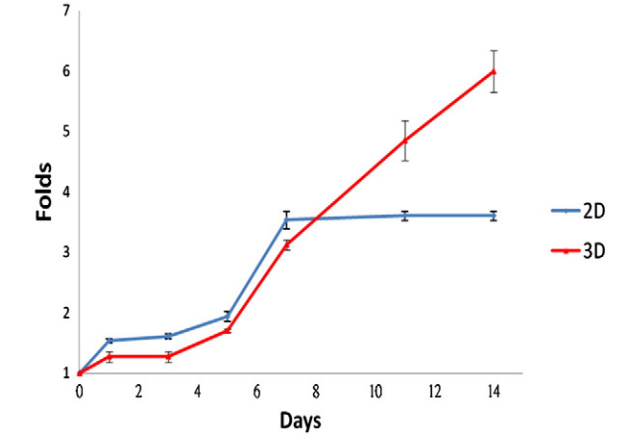

	Day1	Day3	Day5	Day7	Day11	Day14
2D (Mean±SD)	1.53±0.04	1.61±0.04	1.94±0.08	3.54±0.14	3.60±0.08	3.62±0.07
3D (Mean±SD)	1.27±0.09	1.27±0.09	1.71±0.02	3.12±0.09	4.86±0.33*	6.00±0.35*

* p<0.05

Figure 1. Cell viability of cardiomyocytes by the WST-1 assay at different culture time points in 2D and 3D system. The experiments were repeated 5 times to get the mean. The cell viability is presented as fold change (mean ± SD) comparing to Day 0. Cardiomyocytes in the 3D scaffold demonstrated an increased proliferation capacity compared with those in the 2D system after Day 11.

Cardiomyocytes in the 2D were observed to attach more closely than in the 3D nanopeptide scaffolds (Figure 2, *A*). The cells were round shape in 2D and elongated, spindle shape in 3D culture (Figure 2, *B*, *C*). However, because of the cells were embedded in gel-like 3D scaffolds and spread stereoscopically, the global alignment and cell-cell interaction of cardiomyocytes in 3D culture are difficult to observe by fluorescence microscope. Thus we used scanning electron microscopy (SEM) to exhibit the cardiomyocyte allocation in 3D nanopeptide scaffolds. Similar to the SEM observation of PuraMatrix in other group,[15] the expected nanofibers of 0.5% PuraMatrix range from 5 to 30 nm, approximate extracellular matrix environment. The cardiomyocytes were truly embedded in the nanopeptide scaffold, spread and contacted each other less orderly (Figure 3). These images proved the nanopeptide scaffold embedded cells in 3D microenvironment.

Cardiomyocyte contraction and measurement of calcium transients

Although the cardiomyocytes remained spontaneous beating in both groups, cardiomyocytes in the 3D group seemed to show an irregular beating frequency when observed by direct microscopy. For further examination, dual excitation fluorescence measurement system (IonOptix) was used to measure intracellular calcium transients of a single cardiomyocyte on culture day 3. The cardiomyocytes in the 2D system retained a consistent beating pattern (Figure 4, *A*); while the cardiomyocytes in the 3D system had irregular beating rhythm (Figure 4, *B*). Further analysis demonstrated that cardiomyocytes in the 3D system had an approximate 1.42-fold increase in basal level of intracellular calcium concentration as compared with the cardiomyocytes from the 2D culture group (Table 1). The amplitude of calcium transient was smaller as well as the duration of calcium transient was longer in 3D cells as compared with those in 2D cells. Additionally, the culture medium of cardiomyocytes from the 3D culture group contained higher BNP levels than did that of cardiomyocytes from the 2D culture group (197.60 ± 57.86 vs. 59.59 ± 12.44 pg/ml, $p < 0.001$). These findings demonstrate that the cardiomyocytes in the 3D culture system show higher basal levels of intracellular calcium and much more irregular beating rhythm.

Cardiomyocyte gene expression profile

Cardiomyocyte gene expression levels corresponding to the T-type calcium channels Cav3.1 and Cav3.2, the L-type calcium channel CANAC1, and the gap junction protein CX 43 were evaluated by mRNA RT-PCR after 3 days in culture (Table 2). Results are expressed as the fold change relative to the expression level of the cardiomyocytes in the standard 2D culture. No significant differences were observed in T-type or L-type calcium channel expression levels between cardiomyocytes from the 3D culture and the 2D control group. CX 43 expression was increased 2.62-fold in the cardiomyocytes from the 3D culture relative to the cardiomyocytes from the 2D culture.

RNA microarray assay was also performed to compare the difference in mRNA expression of genes related to calcium homeostasis between the 2 groups. No significant difference was noted in cell surface calcium-exporting channels such as sodium/calcium exchanger (NCX1) and plasma membrane Ca2+ ATPase (PMCA). The inositol trisphosphate 3 (IP3) receptor remained similar between the 2 groups. However, in cardiomyocytes from the 3D culture group, sarcoendoplasmic reticulum calcium transport ATPase (SERCA) demonstrated a 2.14-fold increase, accompanied by a 2.33-fold increase in the ryanodine receptor 2 (RyR 2) (Table 3).

Immunofluorescence staining of cardiomyocyte gap junctions and sarcomeres

Cardiomyocytes in the 2D and 3D nanopeptide scaffolds were observed to attach, spread, and express markers of cell interaction in a manner characteristic of cardiomyocyte networks. Notably, cardiomyocytes in the 2D system showed stable end-to-end cell junction expression of CX 43, while cardiomyocytes in the 3D system showed more CX 43 located at the side-to-side cell junctions (Figure 2, *B*, *C*). The cardiomyocytes in the 3D system exhibited an abnormal lateral distribution of CX 43.

Discussion

This study demonstrated that nanopeptide scaffold geometric irregularity can induce arrhythmogenic effect on cardiomyocytes. Our hypothesis is that nanopeptides could mimic the extracellular matrix, and irregular nanopeptide alignment would disorder cardiomyocyte arrangement, causing altered cell bioactivity. Previously, 2D substrates containing aligned

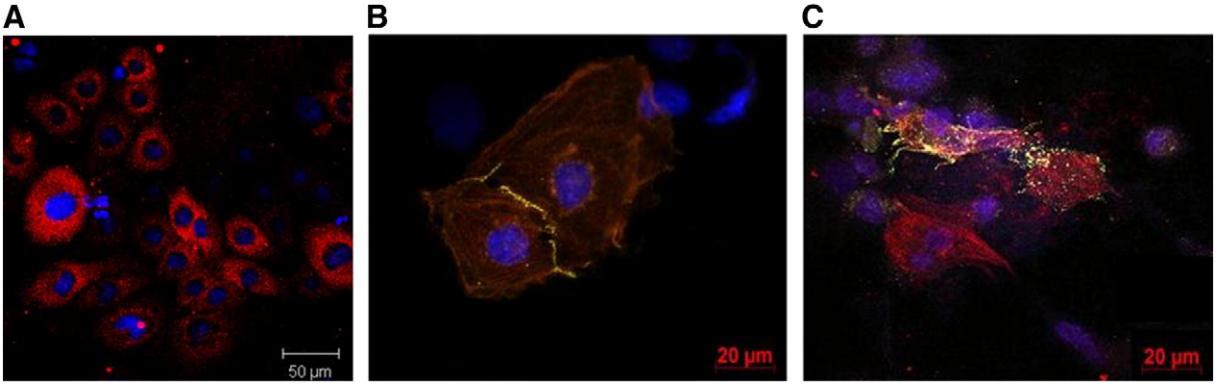

Figure 2. Immunofluorescence image of primary neonatal mouse cardiomyocyte morphology and phenotype after 3 days in culture. Cardiomyocytes contacted closely in 2D system **(A)**. Cardiomyocytes were round shape and connexin 43 located at end-to-end cell junctions in the 2D culture system **(B)**, and were spindle shape in the 3D culture system with lateralization of connexin 43 **(C)**. Yellow, Connexin 43; Red, Troponin I; Blue, DAPI (nuclei).

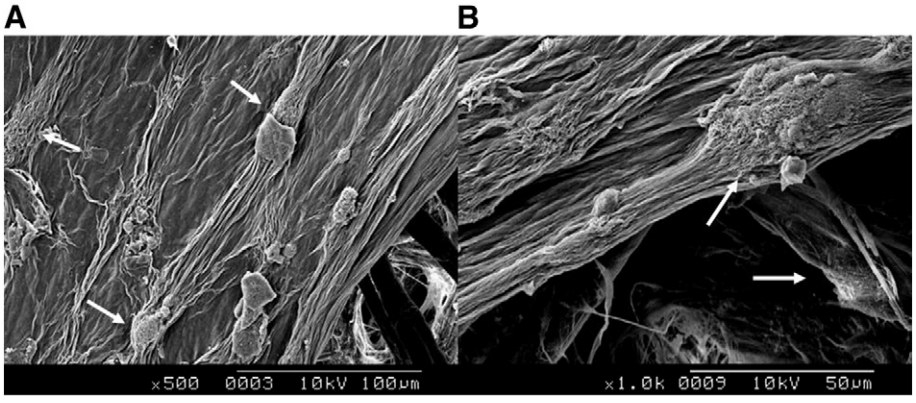

Figure 3. Scanning electron microscopy of the cardiomyocytes in BD PuraMatrix hydrogel nanofiber network. The sample was sputtered with gold films and imaged at 10 kV. Cells were embedded in nanopeptide scaffolds (A, 500×) and spread in a true three-dimensional representation (B, 1000×). White arrow: cardiomyocyte.

topographical patterns have been shown to promote cardiomyocyte alignment and sarcomere organization.[16,17] Aligned substrate topologies were shown to induce an increase in cellular anisotropy and alignment, as well as improved metrics of cardiac electrophysiology, such as conduction velocity.[18] Based on these findings, many ordered 3D anisotropic scaffold structures have been designed and used in cardiomyocyte culture. As the native myocardium is anisotropic, scaffold geometric anisotropy is a critical design parameter to induce cell alignment, transcriptomic stability, and subsequent bioactivity.[19] Emily et al revealed that HL-1 cardiomyocytes in anisotropic scaffolds exhibited significantly elevated 3D alignment and earlier spontaneous beating than isotropic scaffold controls did.[20] Therefore, as in diseased heart, the geometrically irregular scaffold design may cause different cardiomyocyte behavior. BD™ PuraMatrix™ Peptide Hydrogel, a fiber network with an irregular pore size of 50–200 nm, nanofibers range from 5 to 30 nm, was chosen to perform the examination. It is a synthetic peptide hydrogel composed of 16 peptides with a repeating sequence of arginine, alanine, aspartate, and alanine (RADARADARADARADA or RAD16) and a composition of more than 99% water. Under physiological conditions with monovalent cations, the peptide component self-assembles into a 3D hydrogel that exhibits a water–soluble β-sheet nanometer-scale fibrous structure with irregular sized holes. Tokunaga et al showed that injection of PuraMatrix containing cardiac progenitor cells at border area of myocardial infarction improved cardiac function. It also to be angiogenic in vivo and had potential to be a graft for cardiac tissue engineering.[21] Although it was shown to be less effective than collagen at supporting the growth of cardiomyocytes because most of the cells were found at the bottom or the surface of the gels.[22] By immersing in medium containing the cardiomyocytes while forming PuraMatrix gelation, the cardiomyocytes were embedded inside the gel and spread more homogenously in our study.

The nanopeptide hydrogel scaffolds support long-term cardiomyocyte attachment, expansion, and proliferation. While cardiomyocytes in 2D gelatin and gelatin/fibronectin-coated plates gradually reach the proliferation limit, they attached efficiently and persistently spread within the 3D scaffold network. Therefore, the 3D culture system is a suitable method to obtain high cell numbers of cardiomyocytes in culture.

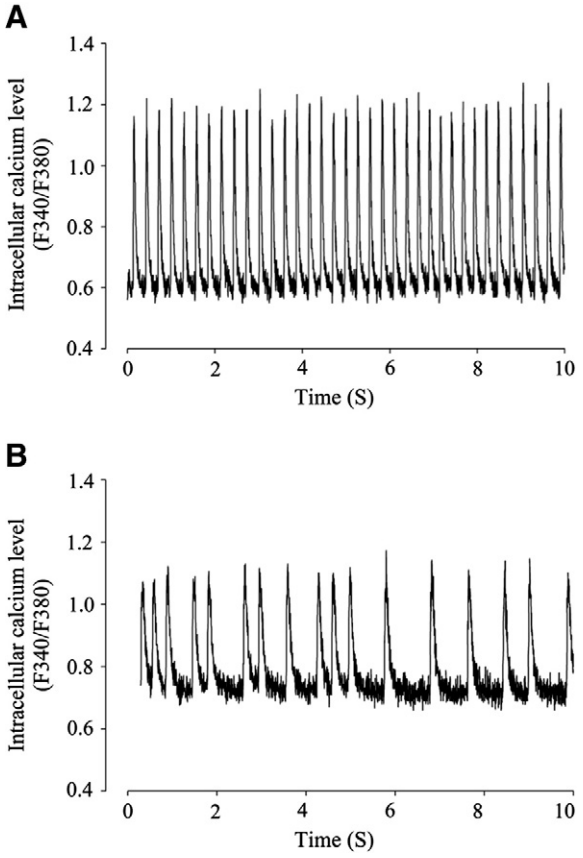

Figure 4. Spontaneous intracellular calcium transients of primary mouse neonatal cardiomyocytes in the 2D and 3D culture system. The tracing shows calcium (Ca2+) transients of cardiomyocytes. Ca2+ transients were expressed as Ca2+ ratiometric signal (F340/F380) (fluorescence intensity ratio of the resultant fluorescent emission excited at 340 nm to that at 380 nm). Primary mouse neonatal cardiomyocytes had regular beating in the 2D culture surrounding **(A)** and irregular contraction in the 3D hydropeptide nanofiber scaffold **(B)**.

Table 1
Analysis of calcium transients.

	Basal calcium level (fluorescence ratio)	Amplitude of $Ca2^+$ transient	$Ca2^+$ transient duration (sec)
2D (N = 5)	0.561 ± 0.019*	0.568 ± 0.006*	0.29 ± 0.04*
3D (N = 5)	0.795 ± 0.017*	0.132 ± 0.075*	0.62 ± 0.29*

* $p < 0.05$

Interestingly, the cells in this 3D scaffold had irregular spontaneous beating. This finding is different from our previous study by using Go Matrix (Bio-Byblos Biomedical co, Taipei, Taiwan), an non-gel, anisotropic 3-dimensional collagen-GAG scaffold. The cardiomyocytes in that system also had better proliferation curve than 2D culture but remained regular spontaneous beating (data not showed). Those cardiomyocytes in PuraMatrix are assumed to have phenotypic changes.

Further functional calcium handling characterization of the cardiomyocyte was conducted by the dual excitation fluorescence photomultiplier system (IonOptix). After loading the cells with fura-2, the calcium flow and the contraction of a single cell were recorded. Cardiomyocytes in the 3D system demonstrated irregular beating and an approximate 1.42-fold increase in intracellular calcium concentration as compared with cardiomyocytes from the 2D group. The irregular beating rhythm and prolonged interval of calcium transient indicated that these cardiomyocytes in 3D group showed arrhythmic changes. The elevated basal intracellular calcium concentration in cardiomyocyte indicated intracellular calcium overload that could induce triggered activity and rendered the cardiomyocytes arrhythmic. The elevated B-type natriuretic peptide mRNA expression also revealed that cardiomyocytes from the 3D culture were under stress and not functioning appropriately. Proper calcium homeostasis is of paramount importance for normal physiological function of the cardiovascular system. When the balance of intracellular calcium is disrupted, pathological and life-threatening conditions can arise. Calcium homeostasis depends on the balance between calcium release and removal. L-type channels provide the primary signal calcium for cardiac contractility via excitation-contraction coupling. T-type calcium channels are localized to the pacemaker tissue where they play an established role in pacemaker function. Generally T-type calcium channels have less expression and do not involve in contractile function in normal cardiomyocyte. However, accumulating evidence supports that T-type calcium channels are re-expressed in cardiomyocytes in cardiovascular disease and injury.[23–25] T-type Ca2+ currents were observed in ventricular myocytes isolated from a feline model of pressure overload-induced cardiac hypertrophy, and these currents contributed to calcium overload, which led to arrhythmic behavior.[26] Therefore, the variations in T-type and L-type calcium channel expression may occur between the 2 groups. In our examination, the mRNA expression levels of both L-type and T-type calcium channels exhibited no difference between the 2D and the 3D cultures. The expressions of other channels, such as NCX1 and PMCA, were also not elevated. Thus, the elevated intracellular calcium in the cardiomyocytes from the 3D culture was not related to the extracellular entry of calcium or a defect in the removal of calcium from the cytosol. The sarcoplasmic reticulum (SR) plays an important role in homeostasis of intracellular calcium concentration. The SR releases stored calcium into the cytosol while RyR receptors or IP3 receptors are activated, which recycle cytosolic calcium into SR by the SERCA channel. While high intracellular calcium levels could induce the elevation of SERCA mRNA levels, the elevation of RyR 2 receptor expression in the 3D model may expel more calcium from the SR into the cytosol, causing the increase in intracellular calcium concentration and arrhythmic changes. Carolina et al reported that cardiomyocytes showed different morphology between 3D and 2D culture systems. Cardiomyocytes in the 3D culture system had increased mitochondria and myofibrils and less endoplasmic reticulum.[27] In our study, the calcium homeostasis function of the SR also changed in 3D cardiomyocytes, providing further evidence that a culture environment could alter cell phenotype expression involving the calcium homeostasis and SR function.

Table 2
3D/2D primary neonatal mice cardiomyocyte mRNA expression ratio of Cav3.1, Cav3.2, CANA1C, and connexin 43 (CX 43) after 3 days in culture.

	Cav3.1	Cav3.2	CANA1C	CX 43
3D/2D ratio (N = 5)	1.24 ± 0.43	1.01 ± 0.37	1.25 ± 0.51	2.62 ± 0.19

Table 3
3D/2D primary neonatal mice cardiomyocyte mRNA expression ratio of calcium homeostasis-related proteins by RNA microarray assay after 3 days in culture.

Protein (Gene)	NCX1 (SLC8A1)	PMCA (ATP2B1)	SERCA (ATP2A1)	RyR 2 (RyR 2)	IP3 receptor (ITPR3)
3D/2D ratio	1.06	1.14	2.14	2.33	1.33

NCX1, Sodium/calcium exchanger; PMCA, Plasma membrane Ca2+ ATPase; SERCA, Sarcoendoplasmic reticulum (SR) calcium transport ATPase; RyR 2, Ryanodine receptor 2; IP3, Inositol trisphosphate.

Elevated intracellular calcium levels could alter gap junction protein expression and function.[28–30] Gap junction channels comprise a hemichannel composed of 6 transmembrane proteins embedded in the plasma membrane of 1 cell joined in a mirror symmetry with a connexin hemichannel in the opposing cell membrane. Dysfunction of gap junction could desynchronize intercellular calcium transients, disrupt intercellular communication and impede synchronous beating among cardiomyocytes.[31] In ischemic heart disease, arrhythmias are often associated with reduced intercellular communication due to changes in connexin expression and gap junction protein malfunction.[32] Reduced expression and altered distribution of CX 43 have been described in patients with other cardiac diseases that are associated with an increased risk of arrhythmias, such as congestive heart failure, dilated cardiomyopathy, and cardiac hypertrophy.[33,34] In our study, the CX 43 mRNA level was not reduced, but was increased in arrhythmic 3D cardiomyocytes. Additionally, the CX 43 expression was not only located at end-to-end cell junctions but also distributed at side-to-side cell junctions. This "lateralization" phenomenon was also reported in ischemic cardiomyocytes[35] that are involved in the dephosphorylation of CX 43 at different sites.[36,37] Thus, in our study, the cardiomyocytes in the 3D scaffold had elevated basal cytosolic calcium content, increased and abnormally distributed CX 43, which resulted in an arrhythmic change. The cardiomyocytes had pathologic changes similar to ischemic cardiomyocytes. This phenomenon was not previously observed in other 3D culture system for cardiomyocytes, a result most likely caused by the geometric disparity between different scaffolds.

A marked up-regulation of connective tissue growth factor (CTGF) expression in left atrial myocardium was found from patients with atrial fibrillation. This was associated with increased fibrosis and connexin 43 expressions.[38] Cardiomyocytes in normal myocardial tissue are electrically coupled primarily in an end-to-end fashion by intercellular gap-junctional complexes. Reactive fibrosis results in extracellular matrix expansion between myocyte bundles, while reparative fibrosis replaces degenerating myocytes. In arrhythmia patients, increased synthesis and decreased degradation type 1 collagen were found, which imply excessive cardiac fibrosis.[8] Therefore, cardiomyocytes cultured in geometrically irregular scaffold may promote fibrosis by increasing collagen amount. However, no difference of gene expression in collagen synthesis (collagen type I alpha 1, alpha 2) and degradation (matrix metallopeptidase 1, tissue inhibitor of metalloproteinase 1) associated protein was found in our study. The expression level of connective tissue growth factor was also similar in 2D and 3D group (Table 4). Probably the 3 days culture time is too short for fibrosis development. If we cultured the cardiomyocytes longer or co-cultured them with fibroblast, the results of fibrosis markers may differ. Hussain et al reported mono-culture of cardiomyocytes in 3D scaffold resulted in loss of cell polarity and islands of non-coherent contractions. After co-culture with fibroblast, the cardiomyocytes had polarized morphology and synchronized contraction. The connexin 43 expression was higher in co-culture than in mono-culture. They concluded that fibroblast-cardiomyocyte co-cultures model involving large tissue-like cellular networks is a promising system for the maintenance of long-term survival and function of cardiomyocytes.[39] With a different design of disarray scaffold, cardiomyocyte arrhythmic change was shown with mono-culture in this study. The co-culture model could possibly further evaluated in such disarray scaffold system. Currently we did not find increased markers of cardiomyocyte fibrosis in this mono-culture model.

The cardiomyocytes in this study were isolated from neonatal mouse. During normal heart maturation and development, neonatal cardiaomyocytes transition from proliferative phenotype (hyperplastic) to cell growth (hypertrophic) phenotype. The formation of cell-cell and cell-extracellular matrix adhesions are crucial during the hypertrophic phase. In the heart, adhesions provide proper alignment of cardiomyocytes and allow them having coordinated, directional contraction. Disruption of intercellular connectivity is associated with arrhythmia and conduction disturbance.[40] Our study proved this concern and showed that geometrically irregular 3D culture scaffold can induce arrhythmic change of neonatal cardiomyocyte. This result is not reported in other group. While using stem cells for regeneration therapy, the effect of microenvironment on early stage cell differentiation should also be concerned. The variation of 3D gel design could change the cell phenotype, make them differentiate and mature in different directions. It was reported that variation of fibrin gel properties can alter early germ layer development of the embryonic stem cells.[41,42] The role of 3D culture system in mechanical induction of stem cell differentiation should be properly evaluated in cell culture and regeneration therapy.

In conclusion, the 3D hydrogel culture system provided a model for the development of cardiac dysrhythmia. Our results suggest that a geometrically irregular 3D culture scaffold may alter cardiomyocyte alignment, beating, sarcoplasmic reticulum function, intracellular calcium concentration, and gap junction protein expression, and may cause arrhythmic changes of cardiomyocytes. These limitations should be considered during

Table 4
3D/2D primary neonatal mice cardiomyocyte mRNA expression ratio of fibrosis-related proteins by RNA microarray assay after 3 days in culture.

Protein (Gene)	MMP-1 (Mmp1a)	TIMP-1 (Timp1)	COL1A1 (Col1a1)	COL1A2 (Col1a2)	CTGF (Ctgf)
3D/2D ratio	1.34	1.36	1.06	0.96	0.94

MMP-1, Matrix metallopeptidase 1; TIMP-1, Tissue inhibitor of metalloproteinase 1; COL1A1, Collagen type I alpha 1; COL1A 2, Collagen type I alpha 2; CTGF, connective tissue growth factor.

cardiac tissue engineering. This 3D cardiomyocyte culture model will be useful for the design and improvement of engineered tissues for construction of cardiac arrhythmic cell model, tissue engineering applications, regeneration therapy and drug testing.

References

1. Freyman T, Polin G, Osman H, Crary J, Lu M, Cheng L, et al. A quantitative, randomized study evaluating three methods of mesenchymal stem cell delivery following myocardial infarction. *Eur Heart J* 2006;**2**:1114-22.
2. Hofmann M, Wollert KC, Meyer GP, Menke A, Arseniev L, Hertenstein B, et al. Monitoring of bone marrow cell homing into the infarcted human myocardium. *Circulation* 2005;**111**:2198-202.
3. Bruggink AH, van Oosterhout MF, de Jonge N, Ivangh B, van Kuik J, Voorbij RH, et al. Reverse remodeling of the myocardial extracellular matrix after prolonged left ventricular assist device support follows a biphasic pattern. *J Heart Lung Transplant* 2006;**25**:1091e8.
4. Lionetti V, Cantoni S, Cavallini C, Bianchi F, Valente S, Frascari I, et al. Hyaluronan mixed esters of butyric and retinoic acid affording myocardial survival and repair without stem cell transplantation. *J Biol Chem* 2010;**285**:9949-61.
5. Lin YD, Yeh ML, Yang YJ, Tsai DC, Zhu TY, Shih YY, et al. Intramyocardial peptide nanofiber injection improves post-infarction ventricular remodeling and efficacy of bone marrow cell therapy in pigs. *Circulation* 2010;**122**:S132-41.
6. Lo LW, Chen SA. Role of atrial remodeling in patients with atrial fibrillation. *J Chin Med Assoc* 2007;**70**:303-9.
7. Burstein B, Nattel S. Atrial fibrosis: mechanisms and clinical relevance in atrial fibrillation. *J Am Coll Cardiol* 2008;**51**:802-9.
8. Polyakova V, Miyagawa S, Szalay Z, Risteli J, Kostin S. Atrial extracellular matrix remodelling in patients with atrial fibrillation. *J Cell Mol Med* 2008;**12**:189-208.
9. Chiu YW, Lo MT, Tsai MR, Hsu RB, Yu HY, Sun CK, et al. Applying harmonic optical microscopy of spatial alignment of atrial collagen fibers in atrial fibrillation. *PLOS One* 2010;**5**:e13917.
10. Tsai MR, Chiu YW, Lo MT, Sun CK. Second0harmonic generation imaging of collagen fibers in myocardium for atrial fibrillation diagnosis. *J Biomed Opt* 2010;**15**:026002.
11. Gelain F, Bottai D, Vescovi A, Zhang S. Designer Self-Assembling Peptide Nanofiber Scaffolds for Adult Mouse Neural Stem Cell 3- Dimensional Cultures. *PLoS ONE* 2006;**1**:e119.
12. Semino CE, Carlos ES, Joshua RM, Gracy GC. Georgeia Panagiotakis and Shunguang Zhang. Functional differentiation of hepatocyte-like spheroid structures from putative liver progenitor cells in threedimensional peptide scaffolds. *Differentiation* 2003;**71**:262.
13. Semino CE, Kasahara J, Hayashi Y, Zhang S. Entrapment of migrating hippocampal neural cells in 3D peptide nanofiber scaffold. *Tissue Engineering* 2004;**10**:643.
14. Narmoneva DA, Oni O, Sieminski AL, Zhang S, Gertler JP, Kamm RD, et al. Self-assembling short oligopeptides and the promotion of angiogenesis. *Biomaterials* 2005;**26**:4837.
15. Moradi F, Bahktiari M, Joghataei MT, Nobakht M, Soleimani M, Hasanzadeh G, et al. BD PuraMatrix peptide hydrogel as a culture system for human fetal Schwann cells in spinal cord regeneration. *J Neurosci Res* 2012;**90**:2335-48.
16. Zong X, Bien H, Chung CY, Yin L, Fang D, Hsiao BS, et al. Electrospun finetextured scaffolds for heart tissue constructs. *Biomaterials* 2005;**26**:5330e8.
17. Wang PY, Yu J, Lin JH, Tsai WB. Modulation of alignment, elongation and contraction of cardiomyocytes through a combination of nanotopography and rigidity of substrates. *Acta Biomater* 2011;**7**:3285e93.
18. Bursac N, Parker KK, Iravanian S, Tung L. Cardiomyocyte cultures with controlled macroscopic anisotropy: a model for functional electrophysiological studies of cardiac muscle. *Circ Res* 2002;**91**:e45e54.
19. Caliari SR, Weisgerber DW, Ramirez MA, Kelkhoff DO, Harley BAC. The influence of collagen-glycosaminoglycan scaffold relative density and microstructural anisotropy on tenocyte bioactivity and transcriptomic stability. *J Mech Behav Biomed Mater* 2012;**11**:27e40.
20. Gonnerman EA, Kelkhoff DO, McGregor LM, Harley BA. The promotion of HL-1 cardiomyocyte beating using anisotropic collagen-GAG scaffolds. *Biomaterials* 2012;**33**:8812-21.
21. Tokunaga M, Liu ML, Nagai T, Iwanaga K, Matsuura K, Takahashi T, et al. Implantation of cardiac progenitor cells using self-assembling peptide improves cardiac function after myocardial infarction. *J Mol Cell Cardiol* 2010;**49**:972-83.
22. Ikonen L, Kerkelä E, Kujala K, Haaparanta AM, Ahola N, Ellä V, et al. Analysis of different natural and synthetic biomaterials to support cardiomyocyte growth. *Journal of Clinical and Experimental Cardiology* 2001;**S4**:002.
23. Huang B, Qin D, Deng L, Boutjir M, El-Sherif N. Reexpression of T-type Ca2+ channel gene and current in post-infarction remodeled rat left ventricle. *Card Res* 2000;**46**:442-9.
24. Takebayashi S, Li Y, Kaku T, Inagaki S, Hashimoto Y, Kimura K, et al. Remodeling excitation-contraction coupling of hypertrophied ventricular myocytes is dependent on T-type calcium channels expression. *Biochem Biophys Res Commun* 2006;**345**:766-73.
25. Maturana A, Lenglet S, Python M, Kuroda S, Rossier MF. Role of the T-type calcium channel CaV3.2 in the chronotropic action of corticosteroids in isolated rat ventricular myocytes. *Endocrinology* 2009;**150**:3726-34.
26. Nuss H, Houser S. T-type Ca2+ current is expressed in hypertrophied adult feline left ventricular myocytes. *Circ Res* 1993;**73**:777-82.
27. Pontes Soares C, Midlej V, de Oliveira ME, Benchimol M, Costa ML, Mermelstein C. 2D and 3D-organized cardiac cells shows differences in cellular morphology, adhesion junctions, presence of myofibrils and protein expression. *PLoS One* 2012;**7**:e38147.
28. Hossain MZ, Boynton AL. Regulation of Cx43 gap junctions: the gatekeeper and the password. *Science STKE* 2000(54):pe1.
29. Lurtz MM, Louis CF. Intracellular calcium regulation of connexin43. *Am J Physiol Cell Physiol* 2007;**293**:C1806-13.
30. De Vuyst E, Wang N, Decrock E, De Bock M, Vinken M, Van Moorhem M, et al. Ca2+ regulation of connexin 43 hemichannels in C6 glioma and glial cells. *Cell Calcium* 2009;**46**:176-87.
31. Oyamada Y, Zhou W, Oyamada H, Takamatsu T, Oyamada M. Dominant-negative Connexin43–EGFP inhibits calcium-transient synchronization of primary neonatal rat cardiomyocytes. *Exp Cell Res* 2002;**273**:85-94.
32. Beardslee MA, Lerner DL, Tadros PN, Laing JG, Beyer EC, Yamada KA, et al. Dephosphorylation and intracellular redistribution of ventricular connexin43 during electrical uncoupling induced by ischemia. *Circ Res* 2000;**87**:656-62.

33. Severs NJ, Bruce AF, Dupont E, Rothery S. Remodelling of gap junctions and connexin expression in diseased myocardium. *Cardiovasc Res* 2008;**80**:9-19.
34. Saffitz JE, Schuessler RB, Yamada KA. Mechanisms of remodeling of gap junction distributions and the development of anatomic substrates of arrhythmias. *Cardiovasc Res* 1999;**42**:309-17.
35. Kleber AG, Rudy Y. Basic mechanisms of cardiac impulse propagation and associated arrhythmias. *Physiol Rev* 2004;**84**:431-88.
36. Lampe PD, Cooper CD, King TJ, Burt JM. Analysis of Connexin43 phosphorylated at S325, S328 and S330 in normoxic and ischemic heart. *J Cell Sci* 2006;**119**:3435-42.
37. Solan JL, Lampe PD. Key connexin 43 phosphorylation events regulate the gap junction life cycle. *J Membr Biol* 2007;**217**:35-41.
38. Adam O, Lavall D, Theobald K, Hohl M, Grube M, Ameling S, et al. Rac1-Induced Connective Tissue Growth Factor Regulates Connexin 43 and N-Cadherin Expression in Atrial Fibrillation. *J Am Coll Cardiol* 2010;**55**(5):469-80.
39. Hussain A, Collins G, Yip D, Cho CH. Functional 3-D cardiac co-culture model using bioactive chitosan nanofiber scaffolds. *Biotechnol Bioeng* 2013;**110**(2):637-47.
40. Evans HJ, Sweet JK, Price RL, Yost M, Goodwin RL. Novel 3D culture system for study of cardiac myocyte development. *Am J Physiol Heart Circ Physiol* 2003;**285**(2):H570-8.
41. Jaramillo M, Singh S, Velankar S, Kumta PN, Banerjee I. Inducing endoderm differentiation by modulating mechanical properties of soft substrates. *J Tissue Eng Regen Med* 2012 [Epub ahead of print]. http://dx.doi.org/10.1002/term.1602.
42. Zhang X, Jaramillo M, Singh S, Kumta P, Banerjee I. Analysis of regulatory network involved in mechanical induction of embryonic stem cell differentiation. *PloS one* 2012;**7**(4):e35700.